

Vortex Redistribution below the First-Order Transition Temperature in the β -Pyrochlore Superconductor KOs_2O_6

T. Shibauchi,^{1,2} M. Konczykowski,² C. J. van der Beek,² R. Okazaki,¹ Y. Matsuda,^{1,3}
J. Yamaura,³ Y. Nagao,³ and Z. Hiroi³

¹*Department of Physics, Kyoto University, Sakyo-ku, Kyoto 606-8502, Japan*

²*Laboratoire des Solides Irradiés, Ecole Polytechnique, 91128 Palaiseau cedex, France*

³*Institute for Solid State Physics, University of Tokyo, Kashiwa, Chiba 277-8581, Japan*

(Dated: November 5, 2018)

A miniature Hall sensor array was used to detect magnetic induction locally in the vortex states of the β -pyrochlore superconductor KOs_2O_6 . Below the first-order transition at $T_p \sim 8$ K, which is associated with a change in the rattling motion of K ions, the lower critical field and the remanent magnetization both show a distinct decrease, suggesting that the electron-phonon coupling is weakened below the transition. At high magnetic fields, the local induction shows an unexpectedly large jump at T_p whose sign changes with position inside the sample. Our results demonstrate a novel redistribution of vortices whose energy is reduced abruptly below the first-order transition at T_p .

PACS numbers: 74.25.Op, 74.25.Qt, 74.25.Ha, 74.25.Kc

Owing to the competition between vortex interactions, thermal and quantum fluctuations, and the effect of quenched disorder, the physics of type-II superconductors involves a rich discussion on the nature of “vortex matter” [1]. In recent years, much attention has been focused on vortex-lattice melting, which has been found to be a first-order phase transition in high-temperature cuprate superconductors [2, 3, 4, 5]. The first-order transition, vortex pinning, and surface barrier effects are at the origin of nontrivial spatial distributions of the vortex density inside superconductors, which have been the subject of intense research [6, 7, 8].

Very recently, an intriguing first-order transition, completely distinct from vortex lattice melting, has been observed in the vortex state of the β -pyrochlore superconductor KOs_2O_6 , that has a relatively high transition temperature $T_c = 9.6$ K [9, 10]. In this system, a remarkable feature is the anharmonic “rattling” motion of K ions within an oversized Os-O atomic cage [11, 12]; this is believed to be responsible for the unusual convex temperature dependence of the resistivity $\rho(T)$ in the normal state [10]. The first-order transition is manifest through a nearly field-independent peak in the specific heat at $T_p \sim 8$ K [10, 13, 14]. High-field transport measurements have revealed that the concave $\rho(T)$ at high temperatures changes to a T^2 dependence below the first-order transition at T_p [14, 15], suggesting that the phonon spectrum responsible for the anomalous transport properties has a substantial change at T_p . Recent measurements of thermodynamical quantities [14], NMR [16], photoemission [17], and penetration depth [18, 19] suggest superconductivity with strong electron-phonon coupling in this system. The effect of the transition on vortex matter in KOs_2O_6 is of fundamental interest, as this gives one a sensitive probe of the change of the free energy at T_p .

Here, by utilizing a micro-Hall probe magnetometry, we show that the vortex distribution changes in a drastic

way below the first-order transition at T_p . We observe a huge local induction jump, exceeding the global magnetization jump expected from thermodynamics by more than an order of magnitude. This results from a novel vortex redistribution driven by the transition. The formation of this new vortex distribution is a consequence of an abrupt decrease of the vortex line energy below T_p , which is evident from the observed distinct changes of the lower critical field H_{c1} .

KOs_2O_6 single crystals were grown by the technique described elsewhere [10]. Since it has been known that partial hydration diminishes the anomaly in specific heat at T_p , special care was taken to keep the crystals in a dry atmosphere before the measurements. We use a sensitive Hall-sensor array tailored in a GaAs/AlGaAs two dimensional electron gas system. Each sensor has an active area of $6 \times 6 \mu\text{m}^2$, and the center-to-center distance of neighboring sensors is $20 \mu\text{m}$. A KOs_2O_6 crystal with dimensions $110 \times 270 \times 90 \mu\text{m}^3$ is placed on top of the array; the magnetic field H is applied along the $90 \mu\text{m}$ direction by using a low-inductance 1.8-T superconducting magnet with a negligibly small remanent field.

Lower Critical Field.— We first report on results of low-field magnetometry. In Fig. 1 we show the field dependence of local induction $B_{\text{local}}(H)$ measured by the sensor placed close to the center of the crystal in the zero-field cooling (ZFC) condition at $T = 6.4$ K. At very low fields, the sample is in the Meissner state $B_{\text{local}} = 0$ G. Above a first-penetration field $H_{\text{fp}} = 53$ Oe, vortices enter and the induction increases rapidly. By plotting the “local magnetization” defined by $B_{\text{local}} - H$, the first penetration field is more clearly resolved, as a sharp dip with a diverging dB_{local}/dH at H_{fp} . The dip (or peak) positions in the second loop coincide with those in the loop of first magnetization. This behavior strongly suggests that the small overall hysteresis is governed by geometrical (surface) barriers [8, 20] and the contribution of bulk

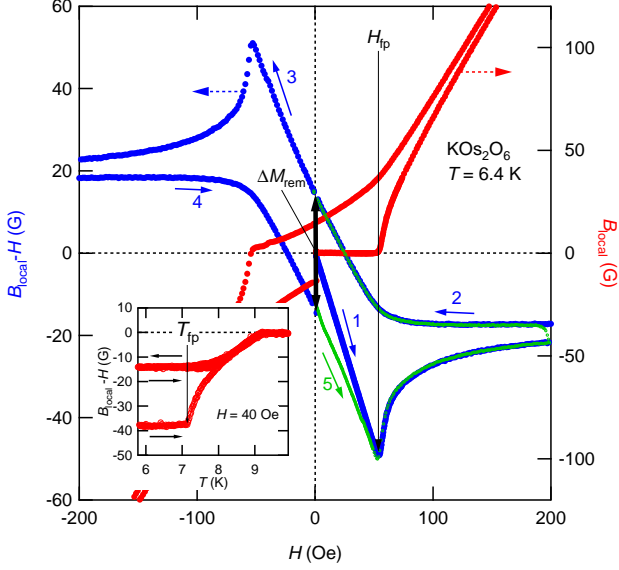


FIG. 1: (color online). Local magnetic induction B_{local} (right axis) and magnetization (left axis) measured at 6.4 K near the sample center as a function of field H . The numbers and thin solid arrows indicate the order and direction of the field sweeps. At the first penetration field H_{fp} , a sharp dip is observed. The remnant magnetization ΔM_{rem} is defined by the hysteresis width at $H = 0$ Oe (thick solid arrow). Inset: the temperature dependence of local magnetization ($H = 40$ Oe) shows a clear kink at the first penetration temperature T_{fp} .

pinning in this system is quite small. Then, the lower critical field H_{c1} can be determined from the expression for the first-penetration field of a superconducting bar, accounting for the demagnetization effect:

$$H_{\text{fp}}/H_{c1} = \tanh(\sqrt{0.36 b/a}), \quad (1)$$

where b/a is aspect ratio of the bar, with the (perpendicular) field along the thickness $2b$ [8].

From Eq. (1), we evaluate $H_{\text{fp}}/H_{c1} = 0.50$ and thus we obtain $H_{c1}(T)$ as depicted in Fig. 2. We also observe a sharp kink at T_{fp} in the temperature dependence of the local magnetization in the ZFC condition as shown in the inset of Fig. 1. These H and T -sweep measurements consistently yield a single $H_{c1}(T)$ curve. Now it is clear that $H_{c1}(T)$ below $T_{\text{fp}} \sim 8$ K is considerably lower than that extrapolated from higher temperature data, although the slope is not very different between above and below T_{fp} . Since the low temperature data extrapolates to a temperature $T_0 = 9.2$ K, clearly lower than T_c , the relative decrease in H_{c1} immediately indicates that the effective transition temperature (*i.e.* the superconducting gap) is reduced below T_{fp} . This concurs with recent microwave penetration depth $\lambda(T)$ -measurements [19], in which a similar shift of the superfluid density $\lambda^{-2}(T)$ to a lower value is observed below T_{fp} . We also note that although a global magnetization measurement [21] gave a

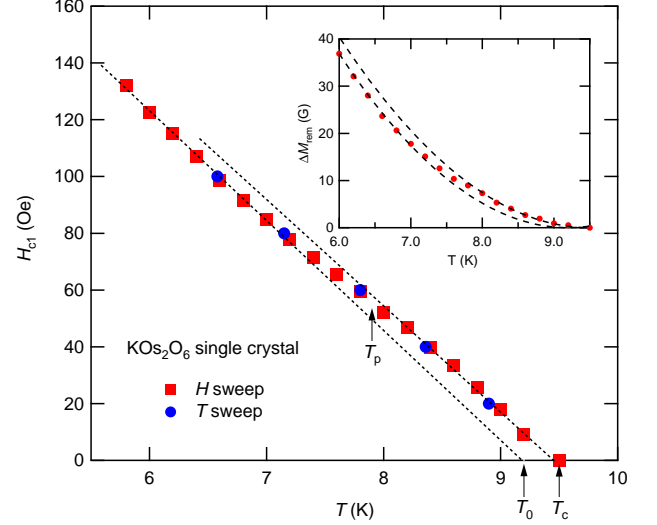


FIG. 2: (color online). Lower critical field as a function of temperature in KOs_2O_6 obtained from the Hall sensor magnetometry. Inset: the temperature dependence of the remnant magnetization. The dotted and dashed lines represent linear and quadratic temperature dependences, respectively.

somewhat smaller value of H_{c1} (5 K), the observed slope $dH_{c1}/dT = -38$ Oe/K near T_c gives a very good agreement with the reported slope values of upper critical field $dH_{c2}/dT = -33$ kOe/K [21, 22] and the thermodynamic critical field $dH_c/dT = -570$ Oe/K through the thermodynamic relation $H_{c1}H_{c2} = H_c^2 \ln \kappa$, where $\kappa \approx 80$ [14, 19] is the Ginzburg-Landau parameter.

A similar feature is seen in the temperature dependence of the remnant local magnetization ΔM_{rem} , defined by the hysteresis width at $H = 0$ Oe [see Fig. 1], which also shows a clear change below T_{p} . As shown in inset of Fig. 2, ΔM_{rem} roughly follows quadratic temperature dependence, but the low temperature data again extrapolate to below T_c . These results all indicate that below T_{p} , the superconducting condensation energy, the effective T_c , and the superconducting gap become smaller than the value extrapolated downward from T_c . According to a recent theory [23], an anharmonic damped phonon mode is responsible for the unusual $\rho(T)$, and its abrupt change from the convex temperature dependence above T_{p} to a T^2 dependence below indicates that the effective phonon frequency is increased dramatically below T_{p} . In this view, the observed reduction of effective T_c implies that the electron-phonon coupling strength is weakened below the first-order transition.

Local Induction Jump.— Next, we turn to the higher field measurements up to 18 kOe. According to the Clausius-Clapeyron relation

$$\Delta B = -4\pi \left(\frac{dT_{\text{p}}}{dH} \right) \left[\Delta S - \Delta V \left(\frac{dT_{\text{p}}}{dp} \right)^{-1} \right], \quad (2)$$

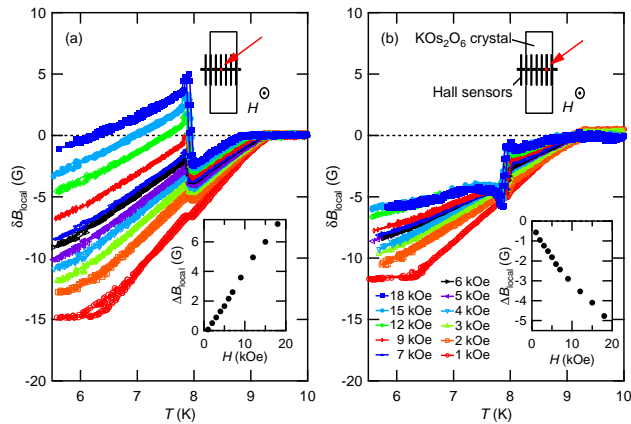


FIG. 3: (color online). Temperature dependence of the local induction change δB_{local} with respect to the value in the normal state, for different applied fields near the crystal center (a) and away from the center (b). The insets show the magnitude of the jump ΔB_{local} at T_p as a function of H .

the first order transition at T_p should be accompanied by a discontinuity ΔB of the global induction (here ΔS is the entropy change per unit volume at the transition, ΔV is the volume change of the sample, and p is pressure). However, given the near-independence of T_p on field and no detectable volume change at T_p by the structural analysis [24], this jump should be modest. From the data of Ref. 14, $\Delta S = 360$ mJ/mol K and $dT_p/dH \approx 0.7$ mK/kOe, the global induction jump at the transition should be ~ 0.4 G. Indeed, recent SQUID measurements give a close value $\Delta B \sim 0.5$ G at 2 T [14], which maintains the thermodynamic consistency.

Surprisingly, however, the local induction $B_{\text{local}}(T)$ reveals a much larger jump at T_p . In Fig. 3(a) we plot the change of the local induction $\delta B_{\text{local}}(T)$ relative to the normal state near the center of the sample. With decreasing temperature, δB_{local} becomes negative below $T_c(H)$ and decreases down to T_p . At T_p , there is a jump with field-dependent magnitude, to the extent that $\delta B_{\text{local}}(T)$ becomes positive at high fields. The magnitude ΔB_{local} of the jump increases linearly with H as shown in the inset; at $H = 18$ kOe it reaches ~ 8 G, which is more than an order of magnitude larger than the global jump.

Most remarkably, the behavior of the ΔB_{local} -jump at T_p strongly depends on the position at which it is measured on the samples. Away from the center, the sign of the induction jump at high fields is reversed as shown in Fig. 3(b): with decreasing temperature $\delta B_{\text{local}}(T)$ decreases abruptly below T_p . Such a position dependence of the magnetization jump is not usually expected for a first-order phase transition. In the first-order vortex lattice melting transition, for example, the induction jump has the same sign everywhere in the sample [6]. This highlights the novelty of the present observation in

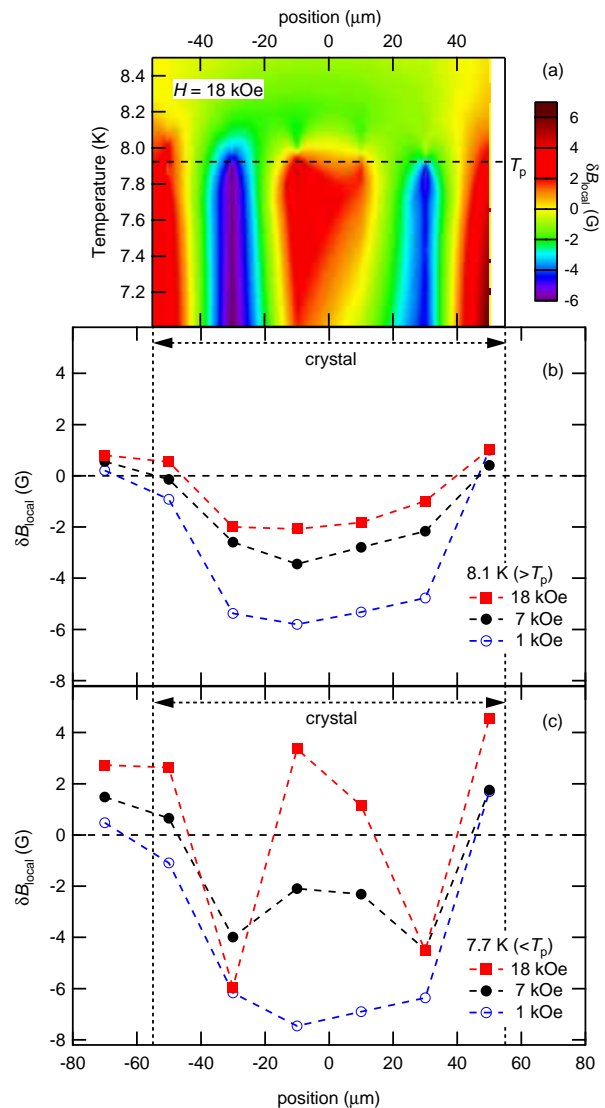


FIG. 4: (color online). Local induction change δB_{local} as a function of position. (a) Contour image of δB_{local} inside the sample at 18 kOe, constituted from interpolations and plotted in the temperature-position plane. This highlights an abrupt change of the vortex distribution near T_p . The position dependence of δB_{local} at several fields is plotted just above (b) and below T_p (c). The dotted lines indicate the approximate positions of the sample edges, and dashed lines are guides to the eye.

KOs_2O_6 . We also note that the observed behavior of $\delta B_{\text{local}}(T)$ is almost reversible with temperature cycles, indicating that bulk pinning by defects does not play a significant role here.

Vortex Redistribution.— To see the anomalous jump at the transition more clearly, we plot the position dependence of δB_{local} in Fig. 4. Above T_p [Fig. 4(b)], the induction profile shows the standard behavior: δB_{local} is negative inside the sample and the difference between

B_{local} and H shrinks with increasing field. We note that the positive δB_{local} near the edges is due to the stray fields by the shielding supercurrent, which are expected for the sample with a finite demagnetizing factor. It should be also noted that the local induction B_{local} inside the sample except for the thin regions near the edges should be equal to $n_v \Phi_0$, where n_v is the density of vortices and Φ_0 is the flux quantum [4]. Just below T_p , the field distribution drastically changed especially at high fields [Fig. 4(c)]. Near the center, the induction jumps to a higher value, while away from the center, it jumps to a lower value. Correspondingly, the vortex density profile now has a characteristic dome-like shape with troughs away from the center. The overall shape remains unchanged down to low temperature [Fig. 4(a)]. A somewhat similar dome shaped field profile has been studied for thin high- T_c cuprate crystals at high temperature and low magnetic fields, where geometrical barriers against flux entry govern the vortex distribution [20]. In contrast, our results are obtained in a field range much higher than H_c , where such barrier effects may not be important.

Next we discuss the possible mechanism of this novel vortex redistribution below T_p . Since we experimentally observe the reduced H_{c1} below T_p [Fig. 2], the free energy of a single vortex per unit length

$$\varepsilon = \left(\frac{\Phi_0}{4\pi\lambda} \right)^2 \ln \kappa = \frac{\Phi_0}{4\pi} H_{c1} \quad (3)$$

should also be smaller in the low-temperature phase. At the first-order transition, the low- T phase and high- T phase coexist, and the region of the low- T phase is invested by “cheaper” vortices with smaller ε . Then vortices near the boundaries between the two phases should be attracted to the low- T phase region. This mechanism promotes inhomogeneous vortex density: denser in the low- T phase and sparse in the high- T phase regions. The difference Δn_v in vortex density between the two phases is determined by the balance of energy gain $\Delta n_v \Delta \varepsilon$ and the kinetic energy loss $\sim (\Delta n_v)^2$ due to the net current tracing the phase boundary. As temperature is lowered, the whole sample is transformed to the low-temperature phase. However, the mutual repulsion between the shielding supercurrent near the crystal edges and this current “string” surrounding the low-temperature phase nucleus prevents the dome-like flux distribution from relaxing. In this way, we may have the dome-shaped vortex distribution resembling the situation discussed in the presence of the geometrical surface barriers [20]. Although a more quantitative theoretical investigation is necessary for the full understanding of the novel vortex redistribution, the energy difference per unit area between low and high- T phases is given by $\Delta \varepsilon B / \Phi_0$, which may be responsible for the observed H -linear dependence of the jump height ΔB_{local} [insets of Fig. 3].

In summary, by using the micro-Hall probe array, we

have measured the local magnetization at the surface of the KOs_2O_6 single crystal presenting a first-order transition within the superconducting state. A number of anomalies associated with the transition have been observed. Below the first-order transition temperature T_p , (i) the lower critical field is shifted down, (ii) the remanent magnetization shows a relative decrease as well, (iii) the local induction reveals huge jumps which depend on the position inside the sample in an unusual way, and (iv) there is an abrupt vortex redistribution into a flux dome, which we believe decorates the nucleating low-temperature phase. Our results indicate that the change in the rattling motion reduces the superconducting critical fields as well as the vortex energy.

We acknowledge fruitful discussion with T. Dahm, R. Ikeda, A. I. Buzdin, and S. Fujimoto. This work was partly supported by Japan-France Integrated Action Program SAKURA from JSPS, and by Grants-in-Aid for Scientific Research of MEXT, Japan. T. S. is also grateful to the hospitality of the LSI people during his stay at Ecole Polytechnique.

-
- [1] G. Blatter, M. V. Feigel'man, V. B. Geshkenbein, A. I. Larkin, and V. M. Vinokur, *Rev. Mod. Phys.* **66**, 1125 (1994).
 - [2] H. Safar *et al.*, *Phys. Rev. Lett.* **69**, 824 (1992).
 - [3] H. Pastoriza, M. F. Goffman, A. Arribère, and F. de la Cruz, *Phys. Rev. Lett.* **72**, 2951 (1994).
 - [4] E. Zeldov *et al.*, *Nature (London)* **375**, 373 (1995).
 - [5] A. Schilling *et al.*, *Nature (London)* **382**, 791 (1996).
 - [6] A. Soibel *et al.*, *Nature (London)* **406**, 282 (2000).
 - [7] M. Marchevsky, M. J. Higgins, and S. Bhattacharaya, *Nature (London)* **409**, 591 (2001).
 - [8] E. H. Brandt, *Phys. Rev. B* **60**, 11939 (1999).
 - [9] S. Yonezawa, Y. Muraoka, Y. Matsushita, and Z. Hiroi, *J. Phys.: Condens. Matter* **16**, L9 (2004).
 - [10] Z. Hiroi, S. Yonezawa, J. Yamaura, T. Muramatsu, and Y. Muraoka, *J. Phys. Soc. Jpn.* **74**, 1682 (2005); Z. Hiroi *et al.*, *J. Phys. Soc. Jpn.* **74**, 3400 (2005).
 - [11] J. Kuneš, T. Jeong, and W. E. Pickett, *Phys. Rev. B* **70**, 174510 (2004); J. Kuneš, and W. E. Pickett, *Phys. Rev. B* **74**, 094302 (2006).
 - [12] J. Yamaura, S. Yonezawa, Y. Muraoka, and Z. Hiroi, *J. Solid State Chem.* **179**, 336 (2006).
 - [13] M. Brühwiler, S. M. Kazakov, J. Karpinski, and B. Batlogg, *Phys. Rev. B* **73**, 094518 (2006).
 - [14] Z. Hiroi, S. Yonezawa, Y. Nagao, and J. Yamaura, *Phys. Rev. B* **76**, 014523 (2007); Z. Hiroi, S. Yonezawa, and J. Yamaura, *J. Phys.: Condens. Matter* **19**, 145283 (2007).
 - [15] Y. Kasahara *et al.*, *Phys. Rev. Lett.* **96**, 247004 (2006).
 - [16] M. Yoshida *et al.*, *Phys. Rev. Lett.* **98**, 197002 (2007).
 - [17] T. Shimojima *et al.*, *Phys. Rev. Lett.* (to be published).
 - [18] I. Bonalde *et al.*, *Phys. Rev. Lett.* **98**, 227003 (2007).
 - [19] Y. Shimono *et al.*, *Phys. Rev. Lett.* **98**, 257004 (2007).
 - [20] E. Zeldov *et al.*, *Phys. Rev. Lett.* **73**, 1428 (1994).
 - [21] G. Schuck, S. M. Kazakov, K. Rogacki, N. D. Zhigadlo, and J. Karpinski, *Phys. Rev. B* **73**, 144506 (2006).

- [22] T. Shibauchi *et al.*, Phys. Rev. B **74**, 220506(R) (2006);
E. Ohmichi, T. Osada, S. Yonezawa, Y. Muraoka, and Z.
Hiroi, J. Phys. Soc. Jpn. **75**, 045002 (2006).
- [23] T. Dahm and K. Ueda, arXiv:0706.4345 (2007).
- [24] J. Yamaura and Z. Hiroi, (unpublished).